IET Microwaves, Antennas & Propagation

Research Article

IET Journals
The Institution of Engineering and Technology

Accelerated simulation-driven design optimisation of compact couplers by means of two-level space mapping

ISSN 1751-8725
Received on 3rd July 2014
Accepted on 18th October 2014
doi: 10.1049/iet-map.2014.0444
www.ietdl.org

Adrian Bekasiewicz[1] ✉, *Slawomir Koziel*[2], *Bogdan Pankiewicz*[1]

[1]*Faculty of Electronics, Telecommunications, and Informatics, Gdansk University of Technology, Gdansk, Poland*
[2]*Engineering Optimization & Modeling Center, Reykjavik University, Reykjavik, Iceland*
✉ *E-mail: adrian.bekasiewicz@eti.pg.gda.pl*

Abstract: In this study, the authors discuss a robust and efficient technique for rapid design of compact couplers. The approach exploits two-level space mapping (SM) correction of an equivalent circuit model of the coupler structure under design. The first SM layer (local correction) is utilised to ensure good matching between the equivalent circuit and the electromagnetic model at the component level. Subsequent global correction allows for accounting the electromagnetic couplings between the components. The important advantage of two-level model correction is that small number of parameter is utilised at each stage, which substantially simplifies and speeds up the parameters extraction procedure. Another advantage is that the local-global SM results in considerably better generalisation capability of the surrogate model (as compared to conventional SM). This leads to improved reliability of the optimisation process and its reduced computational cost. The proposed technique is validated using an example of two compact microstrip rat-race couplers and compared with other surrogate-based optimisation techniques.

1 Introduction

Miniaturisation of microwave/RF section plays a significant role in the design process of contemporary communication systems. The main difficulty lies in miniaturisation of passive components because of the proportionality relation between their dimensions and the operating frequency. Miniaturisation of rat-race couplers (RRC) is especially important as they have a wide range of applications [1] and, at the same time, they are characterised by considerable footprint. In particular, a circumference of a conventional RRC is about 1.5 of the wavelength.

Various techniques for RRC miniaturisation have been presented in the literature; however, an implementation of slow-wave resonant structures (SWRS) may be considered as a dominant one. The replacement of a coupler sections with their corresponding SWRS significantly increase the phase velocity that allows achieving considerable footprint reduction together with a single layer topology [2, 3]. Moreover, the use of SWRSs results in enhanced circuit functionality, for example, by attenuation of unwanted harmonic frequencies [3, 4]. The SWRS is usually designed as a combination of high- and low-impedance transmission lines [2, 5]. Consequently, it can be shaped as required to maximally utilise the interior area of the coupler. On the other hand, utilisation of SWRS cells within the coupler introduces complex and multi-variable topologies, which significantly complicates its design [4, 6]. Accurate performance evaluation of such densely-packed layouts can only be realised through high-fidelity electromagnetic simulations, which is computationally expensive.

Conventional design techniques utilise knowledge-driven design refinement using repetitive parameter-sweeps [6, 7]. This is a time consuming process, which can simultaneously handle only a few design parameters, and, therefore it cannot lead to a genuinely optimum design. Thus, automated numerical optimisation might be the only way for determining optimum dimensions for complex couplers. Unfortunately, direct optimisation using gradient-based [8] or derivative-free [9] algorithms is hindered for such structures because of high computational cost of single EM simulation of the structure but also, even more importantly, because of large number of such simulations required by conventional optimisation techniques.

The difficulties related to high optimisation cost may be partially alleviated using surrogate-based optimisation (SBO) techniques [10]. In SBO, the optimisation burden is shifted to a computationally cheap surrogate model that is iteratively refined in a prediction-correction loop. The surrogate may be constructed from approximation of sampled data acquired from EM-based model [11], or through appropriate correction of an auxiliary low-fidelity model [12]. On the other hand, straightforward application of SBO algorithms such as implicit space mapping (ISM) [13] or sequential space mapping (SSM) [5] for optimisation of compact circuits may not lead to satisfactory results because of complex geometry relations between their individual segments, considerable EM couplings between the cells (not accounted for by equivalent circuit models) leading to poor generalisation of the SM surrogates, as well as by inconvenient manual setup. Utilisation of the aforementioned techniques is especially troublesome if considerable number of parameters have to be accounted for.

In this paper, we introduce a novel local-global space mapping (LGSM) technique, where in a contrary to ISM and SSM the surrogate model is corrected in a two-level framework. Initially, the refinement is carried out at a single component level (local SM). The corrected components are subsequently used at a structure level to form miniaturised coupler design. At this level, the structure dimensions are optimised, and correction is carried out at a structure level (global SM). This leads to excellent generalisation capability of the surrogate, significant reduction of the SM model parameters, and, consequently, more reliable and faster design as demonstrated using two exemplary RRC structures. The method proposed has been also compared with both ISM and SSM indicated its advantages in attempts of designing compact microwave structures. Experimental validation of the technique is also provided.

2 Design of compact microwave rat-race couplers

The techniques for a conventional rat-race coupler design are well founded (see e.g. [1]), unfortunately, they are usually not applicable for miniaturised structures. This is mostly the effect of

simple geometrical relations within a classical circuit that constitute its transmission properties (conventional equal-split RRC is composed of six distributed line sections of 90° electrical length and equal impedance of 70.7 Ω). On the other hand, the design of miniaturised couplers requires substantial effort towards determination of sufficient abbreviations that may be utilised as substitutions of conventional RRC sections. The primary goal is to reduce the length of the distributed line while preserving its electrical properties and, as a consequence, to reduce the overall footprint of a coupler. To date, a number of techniques for hybrid coupler miniaturisation including: multilayer realisations (e.g. [14, 15]), utilisation of a lumped components (e.g. [16, 17]), or implementation of SWRS [18, 19] have been proposed. SWRS are particularly attractive for RRC miniaturisation because of single-layer design [3, 19] high miniaturisation rate in comparison with conventional circuits [5, 6] and low-fabrication cost, to name just a few.

Unfortunately, lack of universal strategies for determining of SWRS component topology significantly hinders their utilisation for the design of compact couplers. Nonetheless, two major approaches for the design of RRC composed of SWRSs are available: (i) experience-based design of the entire structure [20] and (ii) decomposition of a conventional (reference) circuit and substitution of its sections with their corresponding SWRS components [5]. The former technique allows for a construction of novel designs with unusual properties (both geometry- and performance-wise), yet their performance strongly depend on engineering experience. For that reason, the method is prone to failure even if relatively simple designs with only a few independent design variables are considered [21]. The former approach provides initial simplification of the SWRS construction step, as it only needs to mimic the behaviour of a transmission line section of a conventional RRC. Although coupler decomposition and its subsequent reconstruction with SWRS components is a clearly manual step, the risk of design failure in such a scheme is alleviated by a very simple topology of an RRC. Furthermore, a variety of SWRS topologies that may be utilised to mimic the behaviour of conventional transmission lines as well as methods for assessment of the best SWRS realisations for the requirements are already provided in literature (e.g. in [3–5]), which turns the method attractive even for less experienced engineers.

The general flow for the design of a compact RRC based on substitution of decomposed sections of a conventional structure with their corresponding SWRS components may be summarised as follows:

1. Define design specification of a RRC.
2. Design conventional circuit.
3. Decompose coupler into sections that may be substituted with respective perforations.
4. Substitute decomposed sections with suitable SWRS components.
5. Optimise compact circuit to meet design specifications.

The optimisation step significantly influences the overall computational cost of a design process. In this work, we propose a reliable and low-cost design optimisation methodology that exploits a SBO scheme discussed in Section 3. Miniaturisation techniques based on circuit decomposition into transmission lines and their replacement with SWRS components are well established in literature (e.g. [3–5]) thus we omit their detailed description here.

3 Methodology

In this section, we briefly introduce the optimisation concept of a compact couplers constituted by SWRS components. We also formulate an optimisation problem regarded to miniaturised RRC. Moreover we introduce SBO scheme and the LGSM optimisation approach.

3.1 Problem formulation

In general, the optimisation problem of a compact RRC may be formulated as a following non-linear minimisation task

$$\boldsymbol{x}^* = \arg\min_{\boldsymbol{x}} U(\boldsymbol{R}_f(\boldsymbol{x})) \tag{1}$$

where $\boldsymbol{R}_f(\boldsymbol{x})$ is a response vector of a high-fidelity EM model of the coupler. The vector $\boldsymbol{x}$ denotes a set of independent design variables of a circuit under consideration, whereas U is a scalar merit function (e.g. minimax with lower and upper specifications). Normally, problem (1) is constrained with lower and upper bounds for the designable parameters, as well as other constraints, for example, those ensuring geometry relations between individual cells of the structure. For microwave couplers U usually accounts for S-parameters [4], desired coupling level [25], phase difference between selected ports (both accounted for the given operating frequency) [6], or overall footprint of a circuit [18].

3.2 Surrogate-based optimisation

The computational cost of a high-fidelity $\boldsymbol{R}_f$ model evaluation is too high to attempt solving (1) directly. This is because conventional algorithms [8, 9] require a considerable amount of objective function (and consequently high-fidelity model) evaluations to converge to an optimum solution. The difficulties related to CPU-expensive optimisation may be alleviated by replacing the high-fidelity model $\boldsymbol{R}_f$ with a low-fidelity model $\boldsymbol{R}_c$, for example, in the form of a suitably corrected circuit representation of the respective structure. Formally, the SBO algorithm can be represented using the following iterative procedure [22]

$$\boldsymbol{x}^{(i+1)} = \arg\min_{\boldsymbol{x}} U(\boldsymbol{R}_s^{(i)}(\boldsymbol{x})) \tag{2}$$

that generates approximate solutions $\boldsymbol{x}^{(i)}$ ($i = 0, 1, \ldots$) to the original problem (1). The surrogate at iteration i, $\boldsymbol{R}_s^{(i)}$, is constructed from the low-fidelity model. Typically, surrogate construction aims at ensuring sufficient matching between $\boldsymbol{R}_s^{(i)}$ and $\boldsymbol{R}_f$, at least at and in the vicinity of the current design $\boldsymbol{x}^{(i)}$. Model alignment is normally realised by means of a so-called parameter extraction (PE), which is a non-linear minimisation problem by itself [10]. From the computational efficiency standpoint, it is advantageous to create surrogate models by correcting an underlying low-fidelity model (typically, an equivalent circuit). This is because the knowledge about the structure under design embedded in the $\boldsymbol{R}_c$ model usually leads to a fast convergence of the algorithm (2).

A well working SBO algorithm requires only a few iterations to find a satisfactory solution. Also, the high-fidelity model is typically evaluated only once per iteration [22]. Both factors contribute to the overall low optimisation cost compared with conventional methods.

Several SBO approaches including space mapping [10], manifold mapping [23], or shape preserving response prediction [24], are available for solving microwave and antenna design problems. On the other hand, application of SBO scheme for the design of a compact RRC structure with a complex topology is a challenging task. As mentioned before, the reason is relatively large number of independent design parameters that have to be accounted during optimisation as well as problems with accounting for couplings between respective SWRS components within a circuit. Moreover, complex design also introduces difficulties with PE [4]. Additional problem is poor generalisation capability of the SBO model, which is a consequence of performing PE only for a single (normally, the most recent) iteration point. In such a scheme, $\boldsymbol{R}_s$ fits the responses of $\boldsymbol{R}_f$ only within a close proximity with current design solution. Another issue is that the most advantageous selection of surrogate model parameters as well as low-fidelity model correction schemes are unknown beforehand (which is a known drawback of especially space mapping technology); both problems lead to possible unbalance between approximation and generalisation

capability of the surrogate, which, in turn, affect convergence properties of the SBO scheme and even its very ability to identify an optimum structure geometry and dimensions.

Difficulties related to SBO performance may be addressed by the utilisation of a LGSM methodology explained in Section 3.3. For more detailed explanation of SBO and construction of a surrogate model using circuit representation, see for example, [5, 12, 13].

3.3 Local-global space mapping

The proposed LGSM approach utilises SM correction at two different levels of the coupler structure. The first (local) layer is applied at the level of SWRS component (a so-called inner level model), whereas the second (global) layer is applied at the level of the entire RRC structure (outer level model). The main goal of inner level correction is to improve the alignment between the circuit (low-fidelity) and the EM (high-fidelity) model of the SWRS component. The outer level correction accounts for the EM couplings between densely packed SWRS components that constitute the coupler. Utilisation of two SM layers significantly simplifies the PE by reducing amount of independent design variables that are used for correcting each model at a time. Consequently, the cost of the design optimisation process using LGSM can be greatly reduced compared with conventional space mapping applied only at the level of the entire structure. Furthermore, the surrogate model generalisation is greatly improved compared with conventional SM.

To formulate the LGSM technique let us assume that $\boldsymbol{R}_{f.\mathrm{swrs}}(\boldsymbol{y})$ is a response of the EM model and $\boldsymbol{R}_{c.\mathrm{swrs}}(\boldsymbol{y})$ denotes response of circuit

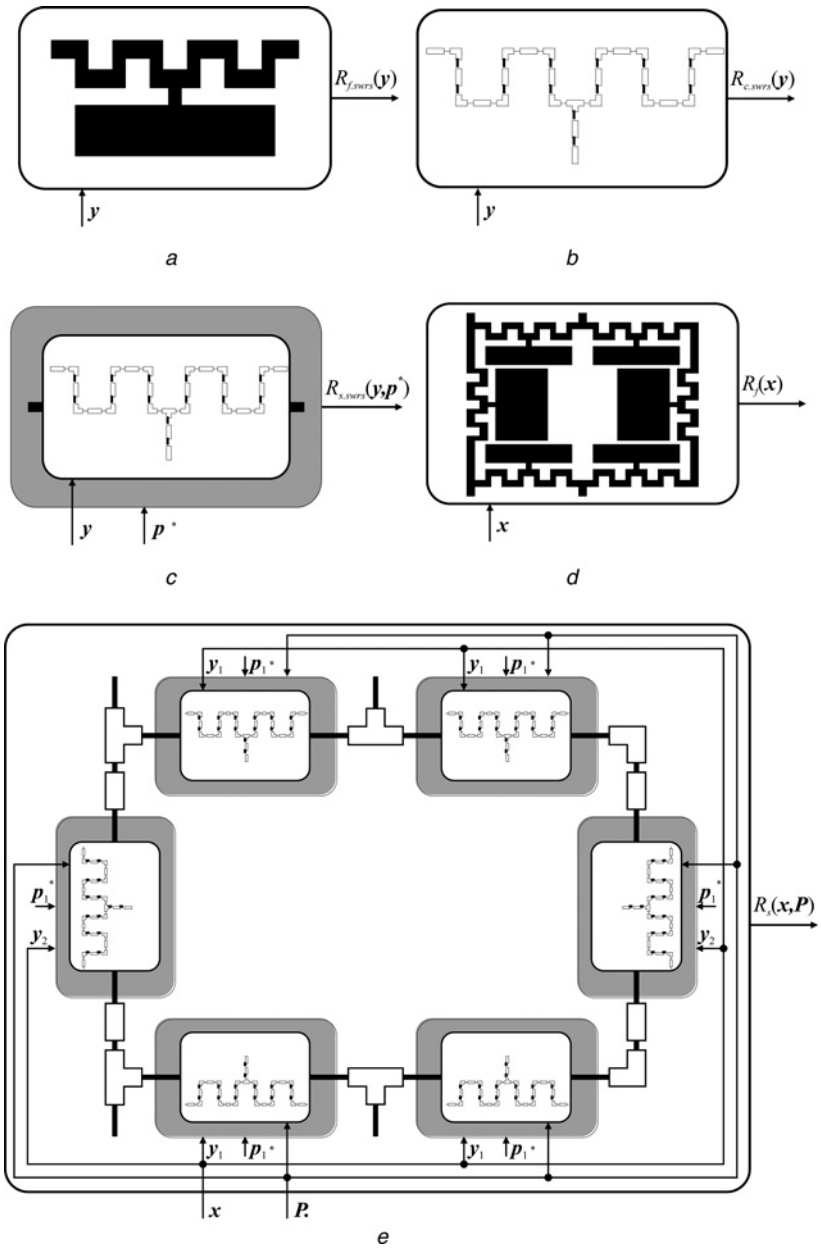

Fig. 1 *Concept of local-global space-mapping (LGSM)*

a High-fidelity (EM)
b Low-fidelity (circuit)
c Inner layer surrogate model of an exemplary SWRS component
A vector $\boldsymbol{y}$ stands for inner layer design variables of SWRS, whereas $\boldsymbol{p}^*$ denotes parameters used during the parameter extraction step
d A high-fidelity model of an exemplary coupler composed of EM models of SWRS components
e The outer layer surrogate model constructed using interconnected inner layer surrogate models of SWRS
Vector $\boldsymbol{x}$ is a concatenation of vectors $\boldsymbol{y}$ (here $\boldsymbol{x} = [y_1, y_2]^T$), whereas $\boldsymbol{P}$ is a vector of perturbations with respect to $\boldsymbol{p}^*$
Here, only one SWRS is utilised for a construction of RRC, thus $\boldsymbol{P} = [p_1^* + d_1]^T$

model of the SWRS component. Here, the vector $\boldsymbol{y}$ stands for the geometry parameters of SWRS. Let $\boldsymbol{R}_{s.\mathrm{swrs}}(\boldsymbol{y})$ denote the surrogate model response of the SWRS component. It is a composition of the low-fidelity model $\boldsymbol{R}_{c.\mathrm{swrs}}(\boldsymbol{y})$ and suitable space mapping corrections aimed at reducing discrepancy between the circuit and EM model responses. A conceptual visualisation of the circuit, the surrogate and the EM models of the SWRS cell is shown in Figs. 1*a*–*c*. The space mapping surrogate $\boldsymbol{R}_{s.\mathrm{swrs}}(\boldsymbol{y})$ of a SWRS component is obtained as

$$\boldsymbol{R}_{s.\mathrm{swrs}}(\boldsymbol{y}) = \boldsymbol{R}_{s.\mathrm{swrs}}(\boldsymbol{y}, \boldsymbol{p}^*) \tag{3}$$

where the vector $\boldsymbol{p}^*$ denotes a set of extractable variables, that is, additional parameters used only at the level of low-fidelity model in order to align it with the high-fidelity representation of the SWRS component. A vector $\boldsymbol{p}^*$ is obtained during a PE procedure by solving the following non-linear minimisation problem

$$\boldsymbol{p}^* = \arg\min_{\boldsymbol{p}} \sum_{k=1}^{N_{\mathrm{swrs}}} ||\boldsymbol{R}_{s.\mathrm{swrs}}(\boldsymbol{y}^{(k)}, \boldsymbol{p}^*) - \boldsymbol{R}_{f.\mathrm{swrs}}(\boldsymbol{y}^{(k)})|| \tag{4}$$

where vectors $\boldsymbol{y}^{(k)}$, ($k = 1, \ldots, N_{\mathrm{swrs}}$) stand for the base solutions for the multi-point PE procedure.

The aim of multi-point parameter extraction is to ensure good generalisation within the entire solution space of the SWRS surrogate model rather than just in the vicinity of any specific design $\boldsymbol{y}$. The solutions are obtained using a star-distribution scheme [10], where $N_{\mathrm{swrs}} = 2r + 1$ (r is a number of independent design variables of the SWRS component). Although the inner layer of each SWRS is described by a much smaller number of extractable parameters than the entire structure of RRC optimised using conventional space mapping technique (usually, up to a few design variables rather than a few dozen variables), it exploits a combination of implicit SM [13], input SM [22] together with frequency scaling [11]. For that reason, a response of a corrected surrogate may be denoted as follows

$$\boldsymbol{R}_{s.\mathrm{swrs}}(\boldsymbol{y}, \boldsymbol{p}^*) = \boldsymbol{R}_{c.F}\left(\boldsymbol{B} \cdot \boldsymbol{x} + \boldsymbol{c}, \boldsymbol{p}_I\right) \tag{5}$$

where $\boldsymbol{B}$ and $\boldsymbol{c}$ are the input SM parameters (here, a diagonal matrix $\boldsymbol{B}$ is exploited). The mapping $\boldsymbol{B}\cdot\boldsymbol{x} + \boldsymbol{c}$ is an affine transformation that modifies the coarse model domain. The entries of the matrix $\boldsymbol{B}$ and the vector $\boldsymbol{c}$ are adjusted using (4) to reduce misalignment between the surrogate and the high-fidelity model. Vector $\boldsymbol{p}_I$ denotes a set of implicit SM [13] parameters (we utilised substrate thickness and permittivity of a microstrip line models) that changes the transmission line properties. Finally, $\boldsymbol{R}_{c.F}$ is a frequency-scaled low-fidelity model $\boldsymbol{R}_{c.\mathrm{swrs}}$. Assuming that $\boldsymbol{R}_{c.\mathrm{swrs}}(\boldsymbol{x}) = \boldsymbol{R}_{c.\mathrm{swrs}}(\boldsymbol{x};\Omega)$, where Ω denotes explicit dependence of the model on frequency (e.g. a discrete frequency sweep), the frequency-scaled model is defined as $\boldsymbol{R}_{c.F}(\boldsymbol{x}), = \boldsymbol{R}_{c.\mathrm{swrs}}(\boldsymbol{x};\Omega')$, where

$$\Omega' = f_0 + f_1\Omega \tag{6}$$

with f_0 and f_1 being the frequency scaling coefficients, obtained, together with other SM parameters through PE. Frequency scaling is a very convenient way of reducing the frequency shifts often present between the models of various fidelities.

Implementation of the outer level space mapping requires preparation of a fine model $\boldsymbol{R}_f(\boldsymbol{x})$ and surrogate model $\boldsymbol{R}_s(\boldsymbol{x}, \boldsymbol{P})$ of the entire RRC structure. An outer space mapping surrogate $\boldsymbol{R}_s(\boldsymbol{x}, \boldsymbol{P})$ is a composition of interconnected inner surrogates of individual SWRS cells

$$\begin{aligned}\boldsymbol{R}_s(\boldsymbol{x}, \boldsymbol{P}) &= \boldsymbol{R}_s\left([\boldsymbol{y}_1; \ldots; \boldsymbol{y}_n], \boldsymbol{P}\right) \\ &= F\left(\boldsymbol{R}_{s.\mathrm{swrs}}(\boldsymbol{y}_1, \boldsymbol{p}^*), \ldots, \boldsymbol{R}_{s.\mathrm{swrs}}\right. \\ &\quad \left.\times(\boldsymbol{y}_k, \boldsymbol{p}^*), \ldots, \boldsymbol{R}_{s.\mathrm{swrs}}(\boldsymbol{y}_n, \boldsymbol{p}^*), \boldsymbol{P}\right)\end{aligned} \tag{7}$$

where F realises a sufficient connection between SWRS components of a coupler and vector $\boldsymbol{x}$ is a concatenation of their parameter vectors $\boldsymbol{y}_k (k = 1, 2, \ldots, n)$. Moreover, $\boldsymbol{P} = [\boldsymbol{p}_1^* + \boldsymbol{d}_1, \ldots, \boldsymbol{p}_k^* + \boldsymbol{d}_k, \ldots, \boldsymbol{p}_n^* + \boldsymbol{d}_n]^{\mathrm{T}}$ stands for space mapping parameters at the outer level and it is defined as a perturbation $\boldsymbol{d}_k$ with respect to $\boldsymbol{p}_k^*$. For the outer layer surrogate $\boldsymbol{R}_s$, we only use frequency and implicit SM. It should be emphasised that perturbations $\boldsymbol{d}_k$ are utilised only to account for couplings between densely allocated SWRSs. Moreover, the range of $\boldsymbol{d}_k$ is normally small (usually up to 10% of $\boldsymbol{p}_k^*$), which is sufficient because of good generalisation of the surrogate constructed with the inner SM layer. The outer level surrogate model at ith iteration of (2) is represented by $\boldsymbol{R}_s^{(i)}(\boldsymbol{x}) = \boldsymbol{R}_s(\boldsymbol{x}, \boldsymbol{P}^{(i)})$, where the global SM parameters $\boldsymbol{P}^{(i)}$ are extracted to minimise $||\boldsymbol{R}_s(\boldsymbol{x}^{(i)}, \boldsymbol{P}) - \boldsymbol{R}_f(\boldsymbol{x}^{(i)})||$. It should be emphasised that in LGSM approach, only one design at the outer space mapping layer is utilised for parameter extraction process which is because of good alignment between SWRS surrogate models provided by the inner layer. The models $\boldsymbol{R}_s(\boldsymbol{x}, \boldsymbol{P})$ and $\boldsymbol{R}_f(\boldsymbol{x})$ are illustrated in Figs. 1*d* and *e*, respectively. The algorithm may be summarised as follows:

1. Construct the circuit model $\boldsymbol{R}_{c.\mathrm{swrs}}$ and the EM model $\boldsymbol{R}_{f.\mathrm{swrs}}$ of each SWRS component.
2. Generate base (training) designs using a star-distribution scheme; acquire $\boldsymbol{R}_{f.\mathrm{swrs}}$ data.
3. Obtain the inner space mapping surrogate $\boldsymbol{R}_{s.\mathrm{swrs}}$ of each SWRS by performing multi-point PE of $\boldsymbol{p}^*$ parameters using input SM, implicit SM and frequency scaling.
4. Utilise prepared $\boldsymbol{R}_{s.\mathrm{swrs}}$ components to construct an outer level space mapping surrogate $\boldsymbol{R}_s(\boldsymbol{x}, \boldsymbol{P})$ of the RRC.
5. Utilise SBO with implicit and frequency SM for a coupler optimisation at the outer level model.

4 Case studies

In this section, we provide numerical verification of the LGSM methodology introduced in Section 3. The operation and performance of our technique is demonstrated using two examples of compact RRC constituted by SWRS components. Both structures are required to fulfil the following design specifications:

(i) At least 20% bandwidth defined for both isolation $|S_{41}| \leq -20$ dB and $|S_{11}| \leq -20$ dB.
(ii) 3 dB coupling.
(iii) At least 80% area reduction in comparison with a conventional rectangle-based RRC.

The operating frequency is set to 1 GHz. The couplers are designated to operate on Taconic RF-35 dielectric substrate ($\varepsilon_r = 3.5$, $\tan\delta = 0.0018$, $h = 0.762$). A comparison of the LGSM technique with benchmark methods is also provided.

4.1 Reference coupler

Let us consider a conventional rectangle-shape, equal-split RRC [25]. A circuit is constructed using well-known even-odd mode analysis [1]. Physical dimensions of each section of a coupler are represented by a vector $\boldsymbol{x}_r = [0.87\ 45.8]^{\mathrm{T}}$, whereas dimensions of the feeding ports $l_0 = 10$, $w_0 = 1.7$ are fixed to ensure 50 Ω input impedance (all dimensions in mm). One should emphasise that the design is characterised by a considerable footprint of ~4536 mm^2 (47.5 × 95.5 mm^2).

4.2 Coupler I

Consider a structure of an equal-split compact RRC. The circuit is composed of two vertical and four horizontal SWRS components constituted by interconnection of high-impedance meander lines and low-impedance stubs, which ensures sufficient flexibility of design parameters, important for a circuit miniaturisation [4].

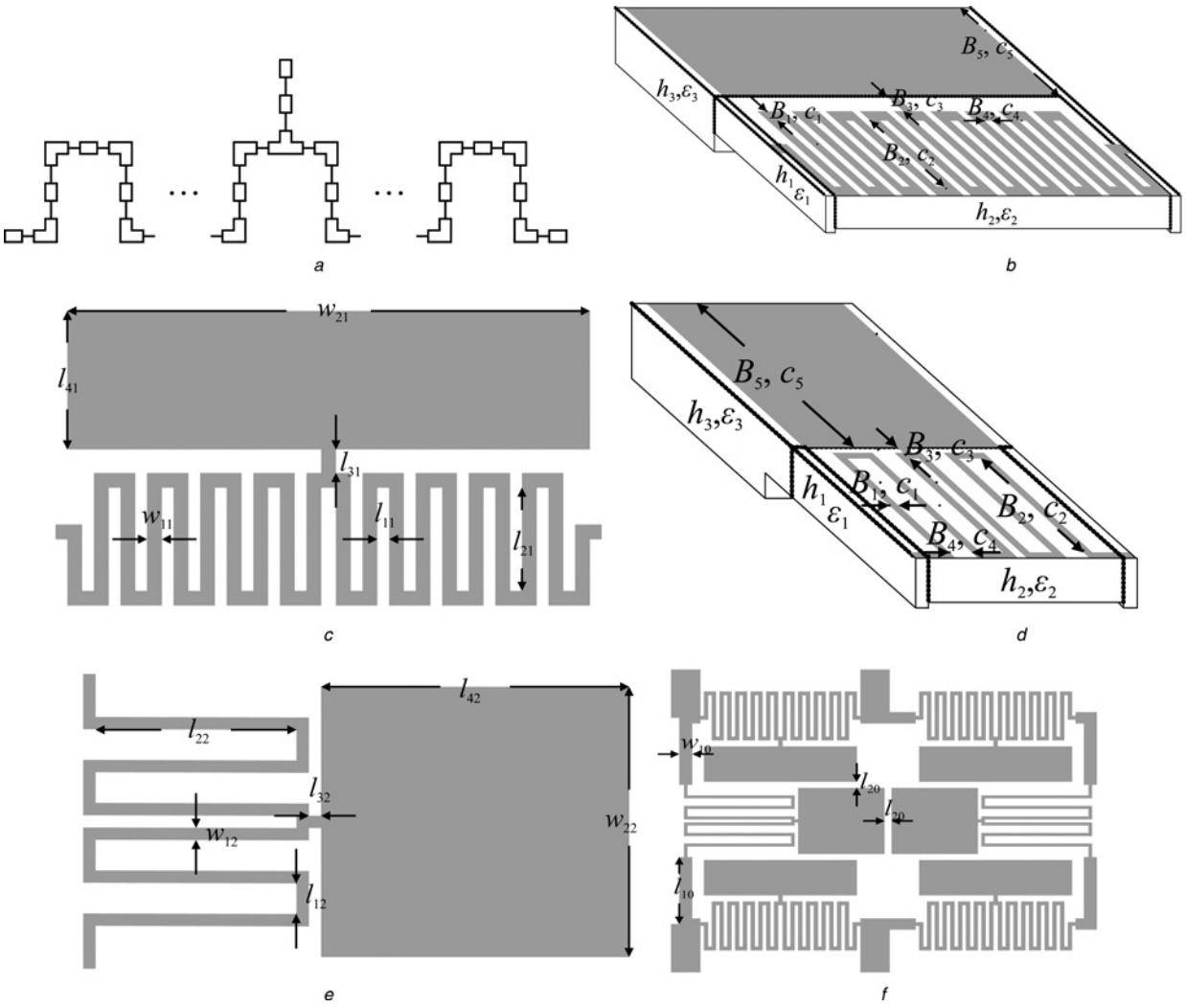

Fig. 2 *Coupler I*

a Generalised low-fidelity model $\boldsymbol{R}_{c.\mathrm{swrs}}^{(1,2)}$
b Visualisation of $\boldsymbol{R}_{s.\mathrm{swrs}}^{(1)}$ with 14 extractable parameters (apart from frequency scaling)
c Geometry of $\boldsymbol{R}_{f.\mathrm{swrs}}^{(1)}$ with highlighted parameters
d Inner layer model of $\boldsymbol{R}_{s.\mathrm{swrs}}^{(2)}$
e Geometry of $\boldsymbol{R}_{s.\mathrm{swrs}}^{(2)}$
f Geometry of a compact coupler

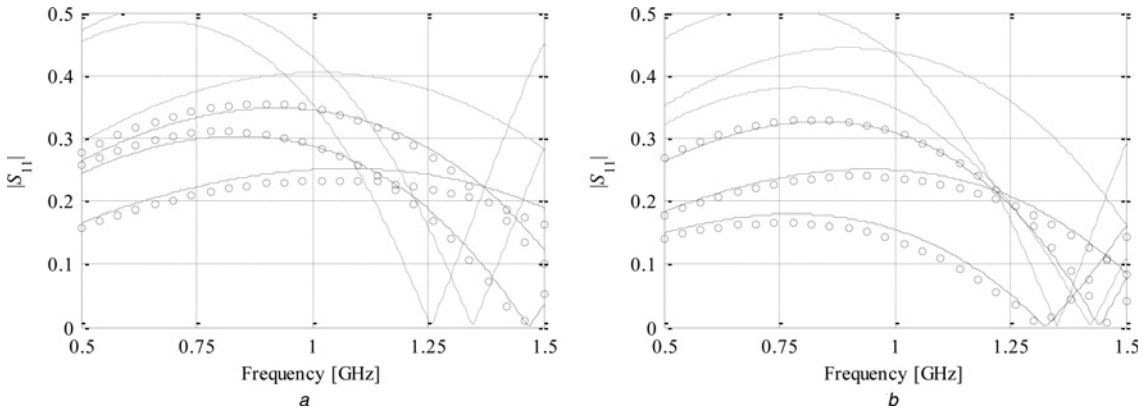

Fig. 3 *Coupler I: responses of the SWRS components at selected 3 of 11 base solutions utilised for multi-point parameter extraction*

a Horizontal SWRS
b Vertical SWRS
Low-fidelity model $\boldsymbol{R}_{c.\mathrm{swrs}}^{(1,2)}$ response (- - - -), high-fidelity $\boldsymbol{R}_{f.\mathrm{swrs}}^{(1,2)}$ model response (——), response of local space mapping surrogate $\boldsymbol{R}_{s.\mathrm{swrs}}^{(1,2)}$ (○○○○).

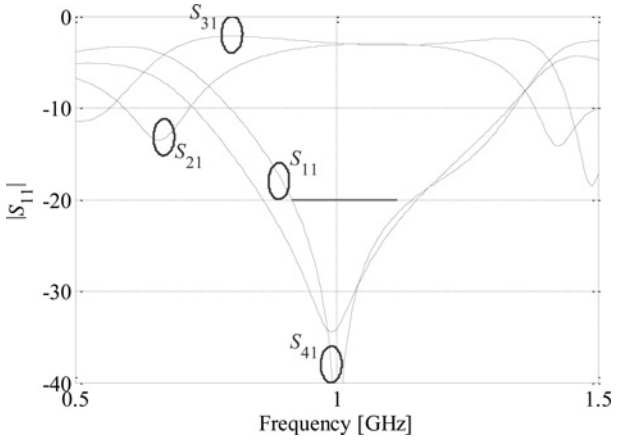

Fig. 4 *Coupler I: simulated transmission characteristics of a miniaturised RRC at the optimised design*

Both SWRS are represented by the following vectors parameters: $\boldsymbol{y}^{(1)} = [w_{11}\ l_{11}\ l_{21}\ l_{31}\ l_{41}]^{\mathrm{T}}$, and $\boldsymbol{y}^{(2)} = [w_{12}\ l_{12}\ l_{22}\ l_{32}\ l_{42}]^{\mathrm{T}}$ (see Figs. 2*c* and *e*). The following lower/upper bounds $\boldsymbol{l}/\boldsymbol{u}$ of each structure dimensions are selected: $\boldsymbol{l}^{(1)} = [0.2\ 0.2\ 0.2\ 0.2\ 0.2]^{\mathrm{T}}$, $\boldsymbol{u}^{(1)} = [0.5\ 0.5\ 4\ 0.5\ 4]^{\mathrm{T}}$, and $\boldsymbol{l}^{(2)} = [0.2\ 0.2\ 0.2\ 0.2\ 0.2]^{\mathrm{T}}$, $\boldsymbol{u}^{(2)} = [0.5\ 1\ 7\ 0.5\ 7]^{\mathrm{T}}$. The low-fidelity models $\boldsymbol{R}_{c.\mathrm{swrs}}^{(1,2)}$ of both structures are constructed in Agilent ADS circuit simulator [26] (see Fig. 2*a*), whereas high-fidelity models $\boldsymbol{R}_{f.\mathrm{swrs}}^{(1,2)}$ of SWRS are both prepared in CST Microwave Studio [27] (~340 000 and ~400 000 mesh cells, as well as 4 and 4.5 min evaluation time for $\boldsymbol{R}_{f.\mathrm{swrs}}^{(1)}$ and $\boldsymbol{R}_{f.\mathrm{swrs}}^{(2)}$, respectively). The inner layer surrogate model $\boldsymbol{R}_{s.\mathrm{swrs}}^{(1)}$, includes: 10 input space mapping (five entries of the matrix $\boldsymbol{B} = \mathrm{diag}([B_1\ B_2\ B_3\ B_4\ B_5]^{\mathrm{T}})$ and five entries of the vector $\boldsymbol{c} = [c_1\ c_2\ c_3\ c_4\ c_5]^{\mathrm{T}}$), six ISM parameters (three substrate heights and three permittivities $\boldsymbol{p}_I = [h_1\ h_2\ h_3\ \varepsilon_1\ \varepsilon_2\ \varepsilon_3]^{\mathrm{T}}$), as well as two frequency scaling (f_0 and f_1) parameters. A star-distribution design of experiments (cf. Section 3.3) has been utilised for generating 11 base points for extraction of the $\boldsymbol{R}_{s.\mathrm{swrs}}^{(1)}$ model parameters. Visualisation of the SWRS model with the emphasis on its

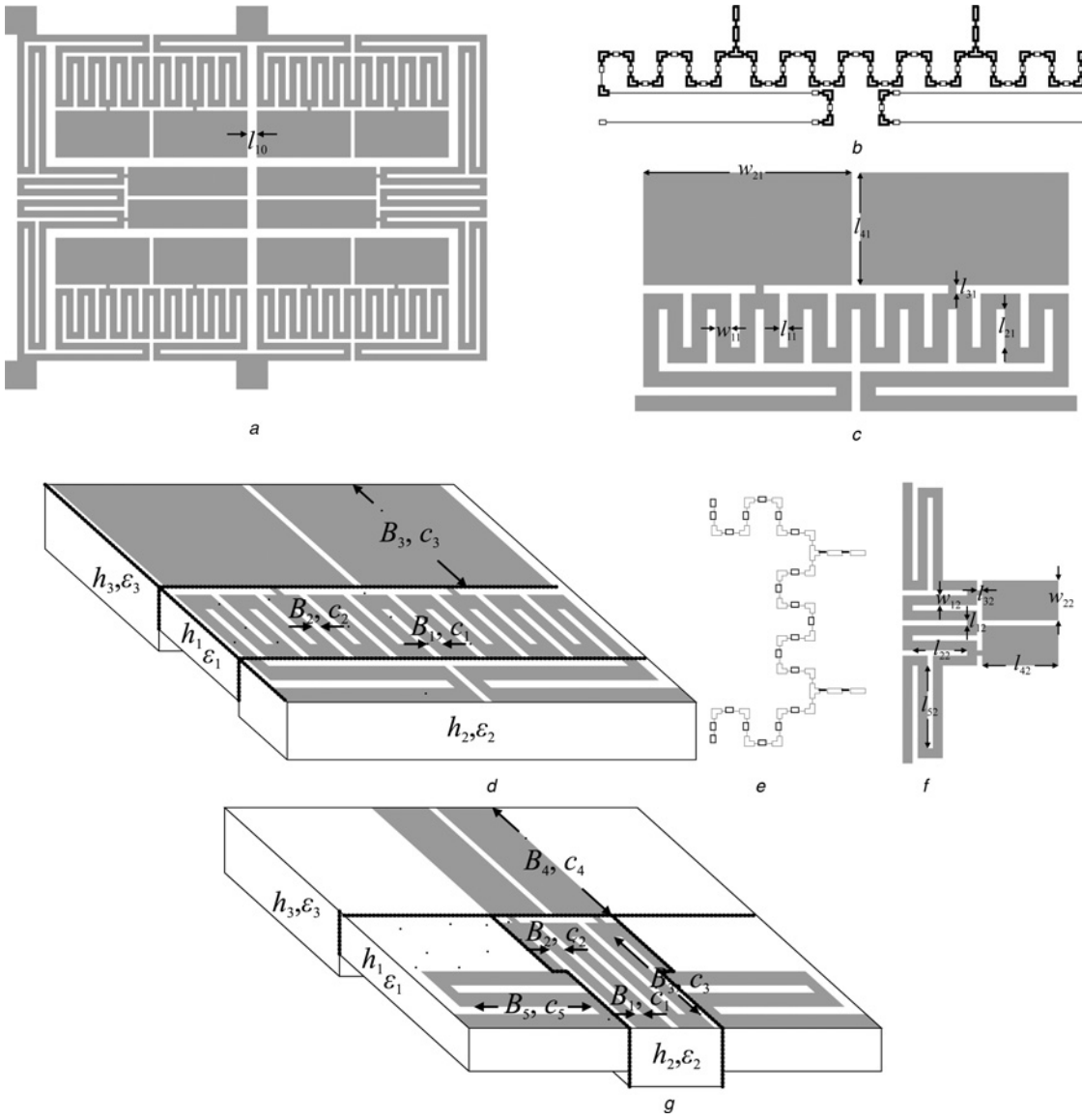

Fig. 5 *Coupler II*

a Geometry
b Equivalent circuit of the horizontal SWRS
c Dimensions of the horizontal component
d Visualisation of $\boldsymbol{R}_{s.\mathrm{swrs}}^{(1)}$ with highlighted extractable parameters
e Equivalent circuit of the vertical SWRS component
f Geometry of the vertical SWRS
g Visualisation of $\boldsymbol{R}_{s.\mathrm{swrs}}^{(2)}$ with highlighted extractable parameters

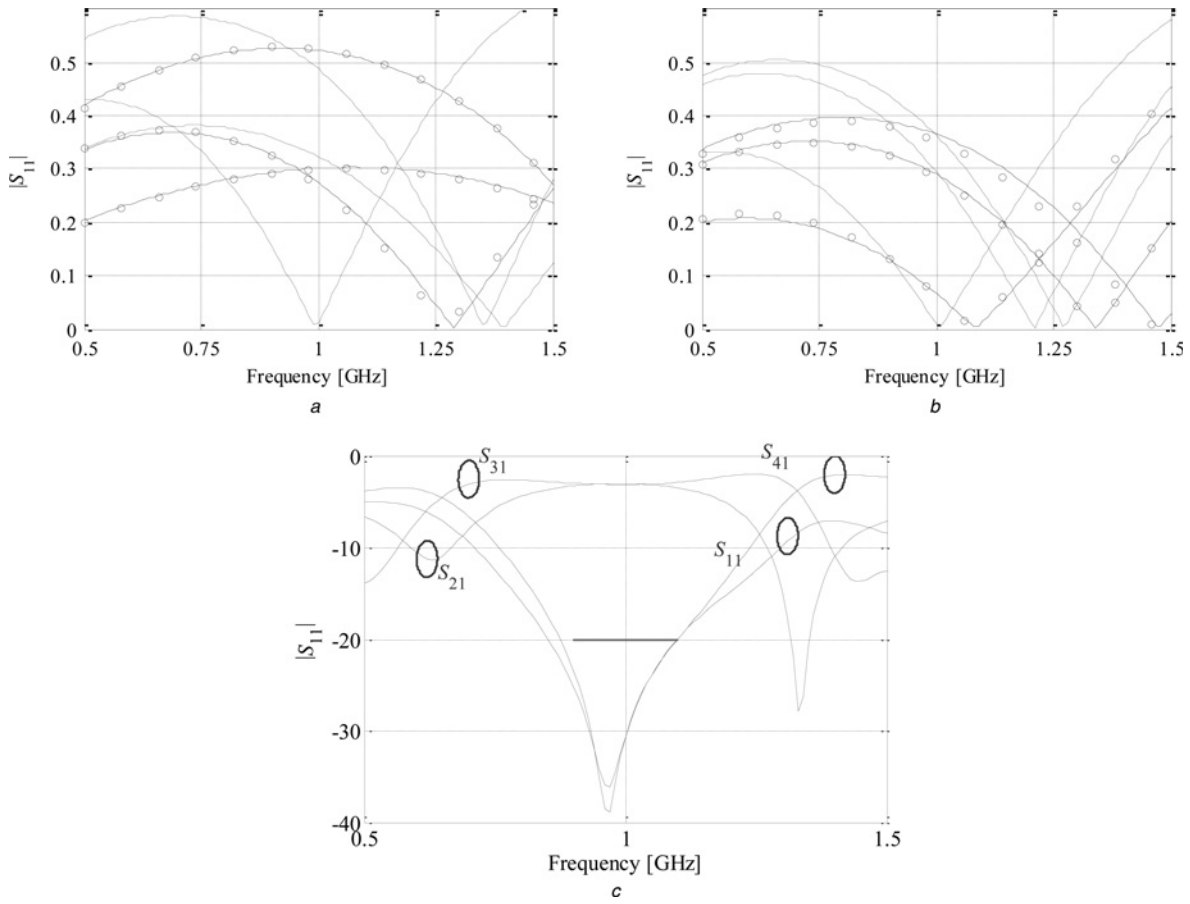

Fig. 6 *Coupler II: responses of the SWRS components utilised for multi-point parameter extraction*

a Horizontal SWRS at 3 of 7 selected designs
b Vertical SWRS at 3 of 11 designs
Coarse model response (- - - -), fine model response (—), response of local space mapping surrogate (○○○○)
c Simulated transmission characteristics at the optimised design

geometrical and extractable parameters is shown in Figs. 2*b* and *c*. A total of 18 extractable parameters (two input SM for each independent design variable, six implicit SM and two for frequency scaling) are also utilised for a construction of the inner-layer surrogate model $\boldsymbol{R}_{s.\mathrm{swrs}}^{(2)}$ (see Fig. 2*d*). Fig. 3 shows a comparison of SWRS model responses before and after multi-point PE.

The vector of coupler dimensions is $\boldsymbol{x} = [w_{11}\ l_{11}\ l_{21}\ l_{31}\ l_{41}\ w_{12}\ l_{12}\ l_{22}\ l_{32}\ l_{42}]^{\mathrm{T}}$, whereas parameters $w_{10} = 0.75$, $l_{10} = 4.3$, $l_{20} = 0.4$ remain fixed. Moreover, $w_{21} = 18l_{11} + 21w_{11}$ and $w_{22} = 6l_{12} + 7w_{12}$ (all parameters in mm). The outer layer surrogate composed of SWRS components (see Fig. 1*e*) and high-fidelity model of the structure (Fig. 2*f*) are prepared with Agilent ADS and CST Microwave Studio (~800 000 mesh cells and simulation time ~75 min per design), respectively. The initial design is $\boldsymbol{x} = [0.2\ 0.2\ 2.5\ 0.2\ 2.5\ 0.2\ 0.2\ 5.0\ 0.2\ 5.0]^{\mathrm{T}}$. The procedure of Section 3.3 is utilised for the design of a coupler. A set of 14 extractable parameters (12 implicit SM defined as perturbations with respect to parameters of individual SWRS component and two frequency scaling ones) are utilised during SBO. A vector of final dimensions: $\boldsymbol{x}^* = [0.24\ 3.35\ 0.26\ 2.04\ 0.28\ 0.25\ 6.52\ 0.29\ 5.63\ 0.29]^{\mathrm{T}}$ is obtained after 4 evaluations of $\boldsymbol{R}_f$ model. The overall footprint of miniaturised RRC is only $17 \times 27.3 = 464\ \mathrm{mm}^2$, thus it offers a considerable miniaturisation of almost 90% with respect to the conventional circuit of Section 4.1. Fig. 4 illustrates transmission characteristics of the miniaturised coupler. One can observe a very slight shift of the operational frequency. The actual obtained −20 dB bandwidth is 23.5%, which is broader than assumed in the specifications. The lower and upper operating frequencies are 0.915 and 1.150 GHz, respectively.

The total design optimisation cost of the structure corresponds to 6.5 $\boldsymbol{R}_f$ simulations (~8.6 h). The cost includes 22 $\boldsymbol{R}_{f.\mathrm{swrs}}$ models evaluations (simulation time corresponding to 1.3 $\boldsymbol{R}_f$) for the generation of the inner space mapping layers of both SWRS components using star-distribution scheme, four $\boldsymbol{R}_f$ simulations for

Table 1 Coupler I (Section 4.2): optimisation cost

Model evaluations	Optimisation algorithm			
	NSM	ISM	SSM	Direct search
SWRS $\boldsymbol{R}_{s.\mathrm{swrs}}$	$0.9 \times \boldsymbol{R}_f$	N/A	N/A	N/A
SWRS $\boldsymbol{R}_{f.\mathrm{swrs}}$	$1.3 \times \boldsymbol{R}_f$	N/A	N/A	N/A
RRC low-fidelity $\boldsymbol{R}_s$	$0.3 \times \boldsymbol{R}_f$	$3.9 \times \boldsymbol{R}_f$	$3.2 \times \boldsymbol{R}_f$	N/A
RRC high-fidelity $\boldsymbol{R}_f$	4	16	12	286
total cost	$6.5 \times \boldsymbol{R}_f$	$18.9 \times \boldsymbol{R}_f$	$15.2 \times \boldsymbol{R}_f$	$286 \times \boldsymbol{R}_f$
total cost, h	8.6	26.5	18.7	363.6

Table 2 Coupler II (Section 4.3): optimisation cost

Model evaluations	Optimisation algorithm			
	NSM	ISM	SSM	Direct search
SWRS $\boldsymbol{R}_{s.\mathrm{swrs}}$	$0.7 \times \boldsymbol{R}_f$	N/A	N/A	N/A
SWRS $\boldsymbol{R}_{f.\mathrm{swrs}}$	$1 \times \boldsymbol{R}_f$	N/A	N/A	N/A
RRC low-fidelity $\boldsymbol{R}_s$	$0.2 \times \boldsymbol{R}_f$	$3.5 \times \boldsymbol{R}_f$	$2.9 \times \boldsymbol{R}_f$	N/A
RRC high-fidelity $\boldsymbol{R}_f$	4	14	11	234
total cost	$5.9 \times \boldsymbol{R}_f$	$17.5 \times \boldsymbol{R}_f$	$13.9 \times \boldsymbol{R}_f$	$234 \times \boldsymbol{R}_f$
total cost, h	5.9	17.5	13.9	234

model refinement after circuit optimisation, as well as the optimisation cost of surrogate models at the inner and outer SM layers (corresponding to about 1.2 simulations of $\boldsymbol{R}_f$ model).

4.3 Coupler II

Consider a novel structure of an equal-split RRC. The design is based on the coupler previously described in [18]. Similarly to the previous example, the circuit is composed of vertical and horizontal SWRS components. Geometry of the structure and both SWRS components with explanation of geometrical parameters is shown in Fig. 5. Both SWRSs are represented by $\boldsymbol{y}^{(1)} = [w_{11}\ l_{11}\ l_{41}]^{\mathrm{T}}$ (Fig. 5*c*), and $\boldsymbol{y}^{(2)} = [w_{12}\ l_{22}\ l_{42}\ l_{52}\ l_{12}]^{\mathrm{T}}$ (Fig. 5*f*). The high-fidelity models $\boldsymbol{R}_{f.\mathrm{swrs}}^{(1,2)}$ of both SWRS components are prepared in CST Microwave Studio [27] (~400 000 mesh cells, 5 min evaluation for $\boldsymbol{R}_{f.\mathrm{swrs}}^{(1)}$ and ~180 000, 2.5 min evaluation for $\boldsymbol{R}_{f.\mathrm{swrs}}^{(2)}$). The low fidelity models (see Figs. 5*b* and *e*) of are prepared in Agilent ADS circuit simulator [26].

The lower/upper bounds are defined by vectors: $\boldsymbol{l}^{(1)} = [0.15\ 0.5\ 0.15]^{\mathrm{T}}$, $\boldsymbol{u}^{(1)} = [0.5\ 3.5\ 0.5]^{\mathrm{T}}$, and $\boldsymbol{l}^{(2)} = [0.15\ 2\ 5\ 1.5\ 0.15]^{\mathrm{T}}$, $\boldsymbol{u}^{(2)} = [0.5\ 5\ 8\ 3.5\ 0.5]^{\mathrm{T}}$. A 7-point PE (cf. Section 3.3) with 14 SM parameters (six for input SM, six for implicit SM and two for frequency scaling) is utilised in order to construct inner SM layer of vertical SWRS component (Fig. 5*d*), whereas inner layer of a horizontal SWRS is generated using 11 base designs and 18 (Fig. 5*g*) SM parameters (ten for input SM, six for implicit SM and two for frequency scaling). A general description of SM parameters is provided in Section 4.2. A comparison between responses of each SWRS for the chosen base solutions before and after PE is illustrated in Figs. 6*a* and *b*.

Both $\boldsymbol{R}_{s.\mathrm{swrs}}$ models have been utilised for a construction of an outer layer surrogate model of compact RRC (see Fig. 1*b*). The

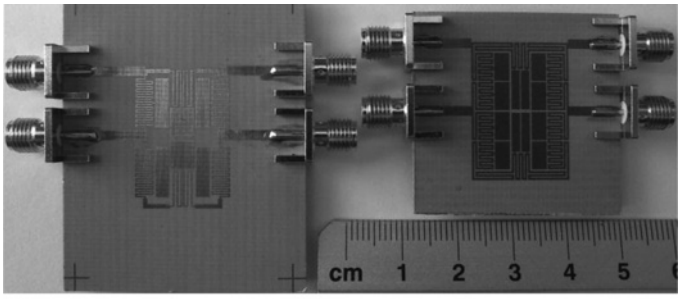

a

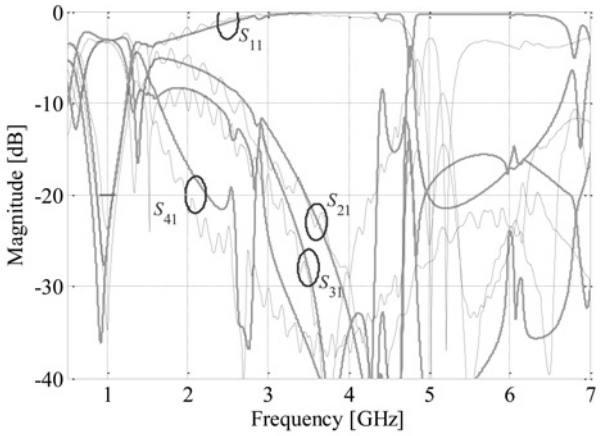

b

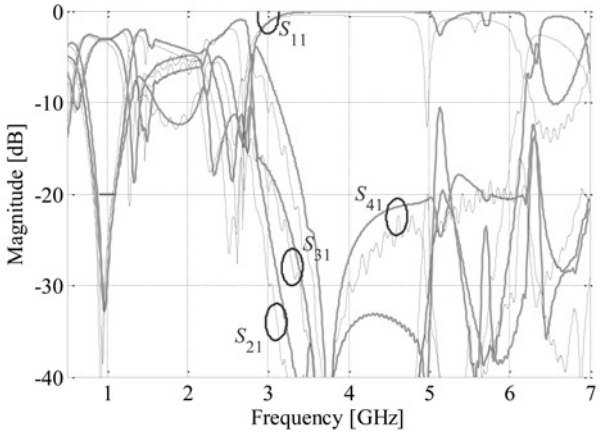

c

Fig. 7 *Experimental verification*

a Fabricated designs: Coupler I of Section 4.2 (left) and Coupler II of Section 4.3 (right); comparison of simulated (grey line) and measured (black line) characteristics
b Coupler I
c Coupler II

structure is constituted by a parameter vector $\boldsymbol{x} = [w_{11}\ l_{22}\ l_{42}\ l_{11}\ l_{41}\ l_{10}]^T$. Variables $w_{12} = w_{11}$, $l_{12} = l_{11}$, $l_{52} = 5w_{11} + 6l_{11} + l_{41}$, $w_{21} = 9w_{11} + 8l_{11}$, $l_{21} = 3w_{11} + 4l_{11}$ and $w_{22} = 3w_{11} + 2l_{11}$. Moreover, upper bound for parameter l_{22} is set to $\boldsymbol{u}^{(2,2)} = \min(5;\ 19w_{11} + 18l_{11} + l_{10} - l_{42})$ in order to prevent overlapping of horizontal SWRS components.

The outer layer surrogate model is prepared in Agilent ADS circuit simulator. The high-fidelity representation of a RRC is constructed in CST Microwave Studio (~600 000 mesh cells and simulation time ~60 min per design). The initial design is: $\boldsymbol{x} = [0.2\ 3\ 5\ 0.2\ 2.5\ 0.2]^T$. A set of 14 extractable parameters (12 implicit SM defined as perturbations and two frequency scaling parameters) is utilised during SBO. Only 4 evaluations of a high-fidelity model were needed for determination of the final coupler dimensions: $\boldsymbol{x}^* = [0.38\ 4\ 7\ 0.2\ 2.72\ 0.32]^T$. An optimised RRC offers 23% bandwidth for the given operating frequency and a considerable miniaturisation of over 90% (overall footprint is $17.4 \times 25.7 = 447\ \text{mm}^2$). Transmission characteristics of optimised design are shown in Fig. 6*c*.

A total aggregated cost of design and optimisation of miniaturised coupler corresponds to 5.9 $\boldsymbol{R}_f$ model evaluations (~5.9 h). Multi-point parameter extraction required 18 $\boldsymbol{R}_{f.\text{swrs}}$ evaluations in total (~1 $\boldsymbol{R}_f$), whereas 4 $\boldsymbol{R}_f$ model simulations were needed for optimisation of a coupler (outer space mapping layer). The cost of surrogate models evaluations ($\boldsymbol{R}_s$, $\boldsymbol{R}^{(1)}_{s.\text{swrs}}$ and $\boldsymbol{R}^{(2)}_{s.\text{swrs}}$) corresponds to about 1.2 simulations of $\boldsymbol{R}_f$ model.

4.4 Comparison with benchmark surrogate-based techniques

Computational efficiency of the proposed LGSM methodology is compared with other competitive SBO methods including ISM [13] and SSM [5], previously utilised for design of compact microwave structures. The method proposed in this work clearly outperforms all the aforementioned techniques. Moreover, a conventional optimisation using a pattern search algorithm [28] has been conducted for both coupler designs. The results indicate that direct high-fidelity model optimisation is virtually impractical for the design of miniaturised RRC structures. A comparison of optimisation methods in terms of computational cost for Coupler I is gathered in Table 1, whereas the design costs for Coupler II are provided in Table 2.

5 Experimental validation

Optimised designs of the couplers considered in Section 4 have been manufactured in order to carry out experimental verification of the proposed optimisation technique. Broadband transmission characteristics of the couplers have been then measured and compared against simulation results.

A photograph of the fabricated circuits and comparison of their transmission characteristics is shown in Fig. 7. Experimental results exhibit very good agreement with the simulations. Moreover, attenuation of harmonic frequencies for both circuits is observed. This phenomenon is introduced by the low-pass filter properties of the SWRS components that constitute miniaturised couplers [3].

6 Conclusion

In this work, a LSGM methodology for fast design of compact microwave couplers is presented. The design technique is based on a decomposition of a conventional coupler and substitution of its transmission line sections with their corresponding SWRS components. The advantage of LGSM technique lies in utilisation of a globally accurate surrogate model, which allows for a substantial design cost reduction. The proposed method has been validated using two exemplary compact RRC structures resulting in optimisation speedup by a factor of 2.75 to 71.5 compared with other state-of-the-art SBO techniques. Good alignment between simulated and measured results demonstrates the correctness of the LGSM technique. Our future research will focus on extension of the technique towards complete automation of the design optimisation process.

7 Acknowledgments

The authors would like to thank Computer Simulation Technology AG, Darmstadt, Germany, for making CST Microwave Studio available.

8 References

1 Pozar, D.M.: 'Microwave engineering' (John Wiley & Sons, 2012, 4th edn.)
2 Wang, J., Wang, B.-Z., Guo, Y.-X., Ong, L.C., Xiao, S.: 'Compact slow-wave microstrip rat-race ring coupler', *Electron. Lett.*, 2007, **43**, (2), pp. 111–113
3 Kurgan, P., Filipcewicz, J., Kitlinski, M.: 'Development of a compact microstrip resonant cell aimed at efficient microwave component size reduction', *IET Microw. Antennas Propag.*, 2012, **6**, (12), pp. 1291–1298
4 Kurgan, P., Bekasiewicz, A.: 'A robust design of a numerically demanding compact rat-race coupler', *Microw. Opt. Technol. Lett.*, 2014, **56**, (5), pp. 1259–1263
5 Bekasiewicz, A., Kurgan, P., Kitlinski, M.: 'New app.roach to a fast and accurate design of microwave circuits with complex topologies', *IET Microw. Antennas Propag.*, 2012, **6**, (14), pp. 1616–1622
6 Tseng, C.-H., Chen, H.-J.: 'Compact rat-race coupler using shunt-stub-based artificial transmission lines', *IEEE Microw. Wirel. Comp. Lett.*, 2008, **18**, (11), pp. 734–736
7 Smierzchalski, M., Kurgan, P., Kitlinski, M.: 'Improved selectivity compact band-stop filter with Gosper fractal-shaped defected ground structures', *Microw. Opt. Technol. Lett.*, 2010, **52**, (1), pp. 227–229
8 Nocedal, J., Wright, S.: 'Numerical optimization' (Springer, 2006, 2nd edn.)
9 Rios, L.M., Sahinidis, N.V.: 'Derivative-free optimization: a review of algorithms and comparison of software implementations', *J. Global Optim.*, 2013, **56**, (3), pp. 1247–1293
10 Bandler, J.W., Cheng, Q.S., Dakroury, S.A., *et al.*: 'Space mapping: the state of the art', *IEEE Trans. Microw. Theory Tech.*, 2004, **52**, (1), pp. 337–361
11 Koziel, S., Bekasiewicz, A., Zieniutycz, W.: 'Expedited EM-driven multi-objective antenna design in highly-dimensional parameter spaces', *IEEE Antennas Wirel. Prop. Lett.*, 2014, **13**, pp. 631–634
12 Koziel, S., Bandler, J.W., Madsen, K.: 'A space mapping framework for engineering optimization: theory and implementation', *IEEE Trans. Microw. Theory Tech.*, 2006, **54**, (10), pp. 3721–3730
13 Bandler, J.W., Cheng, Q.S., Nikolova, N.K., Ismail, M.A.: 'Implicit space mapping optimization exploiting preassigned parameters', *IEEE Trans. Microw. Theory Tech.*, 2004, **52**, (1), pp. 378–385
14 Tseng, C.-H.: 'Compact LTCC rat-race couplers using multilayered phase-delay and phase-advance T-equivalent sections', *IEEE Trans. Adv. Packag.*, 2010, **33**, (2), pp. 543–551
15 Wang, C.-C., Chiu, H.-C., Ma, T.-G.: 'A slow-wave multilayer synthesized coplanar waveguide and its applications to rat-race coupler and dual-mode filter', *IEEE Trans. Microw. Theory Tech.*, 2011, **59**, (7), pp. 1719–1729
16 Xu, H.-X., Wang, G.-M., Zhang, X.-K., Yang, X.-L.: 'Novel compact dual-band rat-race coupler combining fractal geometry and CRLH TLs', *Wirel. Pers. Commun.*, 2012, **66**, (4), pp. 855–864.
17 Hou, J.-A., Wang, Y.-H.: 'Design of compact 90° and 180° couplers with harmonic suppression using lumped-element bandstop resonators', *IEEE Trans. Microw. Theory Tech.*, 2010, **58**, (11), pp. 2932–2939
18 Bekasiewicz, A., Kurgan, P.: 'A compact microstrip rat-race coupler constituted by nonuniform transmission lines', *Microw. Opt. Technol. Lett.*, 2014, **56**, (4), pp. 970–974
19 Kurgan, P., Kitlinski, M.: 'Slow-wave fractal-shaped compact microstrip resonant cell', *Microw. Opt. Technol. Lett.*, 2010, **52**, (11), pp. 2613–2615
20 Awida, M.A., Safwat, A.M.E., El-Hennawy, H.: 'Compact rat-race hybrid coupler using meander space-filling curves', *Microw. Opt. Technol. Lett.*, 2006, **48**, (3), pp. 606–609
21 Eccleston, K.W., Ong, S.H.M.: 'Compact planar microstrip line branch-line and rat-race couplers', *IEEE Trans. Microw. Theory Tech.*, 2003, **51**, (10), pp. 2119–2125
22 Koziel, S., Cheng, Q.S., Bandler, J.W.: 'Space mapping', *IEEE Microw. Mag.*, 2008, **9**, (6), pp. 105–122
23 Echeverría, D., Hemker, P.W.: 'Manifold mapping: a two-level optimization technique', *Comput. Vis. Sci.*, 2008, **11**, (4–6), pp. 193–206
24 Koziel, S.: 'Shape-preserving response prediction for microwave design optimization', *IEEE Trans. Microw. Theory Tech.*, 2010, **58**, (11), pp. 2829–2837
25 Kurgan, P., Kitlinski, M.: 'Doubly miniaturized rat-race hybrid coupler', *Microw. Opt. Technol. Lett.*, 2011, **53**, (6), pp. 1242–1244
26 Agilent ADS, ver. 2011.10, Agilent Technologies, 1400 Fountaingrove Parkway, Santa Rosa, CA 95403-1799, 2011
27 CST Microwave Studio, ver. 2013, CST AG, Bad Nauheimer Str. 19, D-64289 Darmstadt, Germany, 2013
28 Kolda, T.G., Lewis, R.M., Torczon, V.: 'Optimization by direct search: new perspectives on some classical and modern methods', *SIAM Rev.*, 2003, **45**, (3), pp. 385–482